Int. J. Electrochem. Sci., 13 **(2018)** 2286 – 2298, doi: 10.20964/2018.03.29

International Journal of
ELECTROCHEMICAL
SCIENCE
www.electrochemsci.org

Preparation of Molecularly Imprınted Polypyrrole Modified Gold Electrode for Determination of Tyrosine in Biological Samples

Nihal Ermiş[*], *Nihat Tınkılıç*

Ondokuz Mayıs University, Faculty of Science and Letters, Department of Chemistry, Samsun, Turkey
[*]E-mail: nihal.ermis@omu.edu.tr

Received: 5 November 2017 / *Accepted:* 5 January 2018 / *Published:* 5 February 2018

In this paper, a novel electrochemical sensor based on molecularly imprinted polypyrrole film at gold electrode for selective and sensitive detection of tyrosine (Tyr) was fabricated. Tyr was used as template molecule and polymerized in presence of pyrrole, used as the functional monomer. As a comparison a non-modified polymer surface was also prepared under same circumstances without template molecule. The feature of both imprinted and non-imprinted electrode surfaces were performed by cyclic voltammetry (CV), square wave voltammetry (SWV) and electro impedance spectroscopy (EIS). The imprinted polypyrrole sensor exhibited good selectivity toward tyrosine in comparison with other structurally similar molecules. Under the optimal experimental conditions, the linearity range and the detection limit of the imprinted sensor were obtained as $5.0x10^{-9}$–$2.5x10^{-8}$ M and $2.5x10^{-9}$ M, respectively.

Keywords: molecular imprinting, imprinted polymer, polypyrrole, tyrosine

1. INTRODUCTION

Tyrosine is a non-essential amino acid, which is synthesized from phenylalanine. It is vital for herbivores because of being a basic constituent of proteins and precursor of several important compounds, like neurotransmitters including dopamine, nephrine, epinephrine. Elevation of tyrosine plays role in Parkinson's disease, mood disorders and depression. Low levels of tyrosine can cause albinism and alkaptonuria [1,2].

Several techniques have been reported for detection of tyrosine such as high-performance liquid chromatography (HPLC), liquid chromatographic-tandem mass spectrometry (LC-MS), capillary electrophoresis [3-5]. But these methods have some disadvantages like necessity of expensive equipment and complicated sample preparation.

The molecular imprinting method is based on forming polymeric structures in presence of a template molecule. In the synthesis of moleculary imprinted polymers, monomers are polymerized around template molecules, basically. After removing template molecules from the polymeric structure, they leave complementary cavities to their three dimensional structures. Through these cavities molecularly imprinted polymers (MIPs) can be used as selective recognition element [6]. Due to the molecular imprinting technique, substrate selectivity and spesicifity are gained to electrochemical techniques.

Polypyrrole is one of the most frequently used conducting polymer in bioanalytical sensors. In addition to its rapid electrochemical response, low cost, wide dynamic range, low detection limits; it is advantageous due to its capability of imprinting biomolecules at room temperature without denaturation and conformational change [7]. Both low molecular weight molecules like ascorbic acid [8], caffeine [9], paracetamol [10] and high molecular weight molecules like glycoproteins [11] and enzymes [12] can be determined via MIP modified polypyrrole polymer.

In this paper, the fabrication of a highly selective and sensitive tyrosine sensor was investigated using a molecularly imprinted polypyrrole (PPy) polymer film as an artificial recognition element. Pyrrole and tyrosine were used on gold electrode as the functional monomer and template molecule, respectively. Electropolymerization was used to prepare a novel sensor for detecting tyrosine without any extra reagent like enzyme or mediator. As far as we know this is the first application of tyrosine detection, which has been made by using molecularly imprinted polypyrrole without any extra reagent for preparation of the imprinted polymer.

2. MATERIALS AND METHODS

2.1. Materials

All chemicals were used as supplied without further purification and were analytical grade. Pyrrole (Py), potassium ferricyanide ($K_3[Fe(CN)_6]$) and potassium ferrocyanide ($K_4[Fe(CN)_6]$) were purchased from Fisher Scientific, India; potassium chloride, tyrosine and tryptophan, cysteine were purchased from Sigma-Aldrich, USA.

All solutions were prepared with double-distilled water. The solutions were deoxygenated with high purity nitrogen prior to each experiment, which was performed under a nitrogen atmosphere. Distilled water was used for preparation of all solutions and for washing.

2.2. Apparatus

All electrochemical experiments and electropolymerization were performed on a VersaStat 3 electrochemical system (Princeton Applied System) connected to a personal computer. The three-electrode system was consisted of Au (1.6 mm in diameter), Ag/AgCl/KCl(saturated) electrode and Pt wire, as working, reference and the auxillary electrode, respectively. The molecular structure of Tyr imprinted Au electrode was characterized by FT-IR spectrophotometer (Thermo Fisher Scientific,

Nicolet iS10, Waltham, MA, USA). FTIR spectra were scanned in the wave number range from 650 to 4000 cm^{-1}. For surface images, scanning electron microscope was (JEOL USA, Inc.) used.

2.3. Preparation of MIP and NIP electrodes

The surface of the gold electrode was polished on a micro cloth with 1.0 and 0.05 µm aqueous slurry of alumina and it was immersed in an ultrasonic bath in distilled water for 5 min to remove any particles on the surface and then allowed to dry at room temperature. For a cleaner surface, the polished electrode was subjected to cyclic potential sweeping between 0.0 and 1.5 V in 0.5 mol/L sulfuric acid until a stable cyclic voltammogram was obtained. Subsequently, for preparation of MIP, the cleaned electrode was immersed in acetate buffer solution (0.5mol L^{-1}, pH=4) containing 0,06 mol L^{-1} Py and 0,03 mol L^{-1} tyrosine. The electrosynthesis of polypyrrole (PPy) film was performed by cyclic voltammetry (20 scans), between 0 and 1.5 V vs. Ag/AgCl, at a scan rate of 100mV/s (Scheme 1).

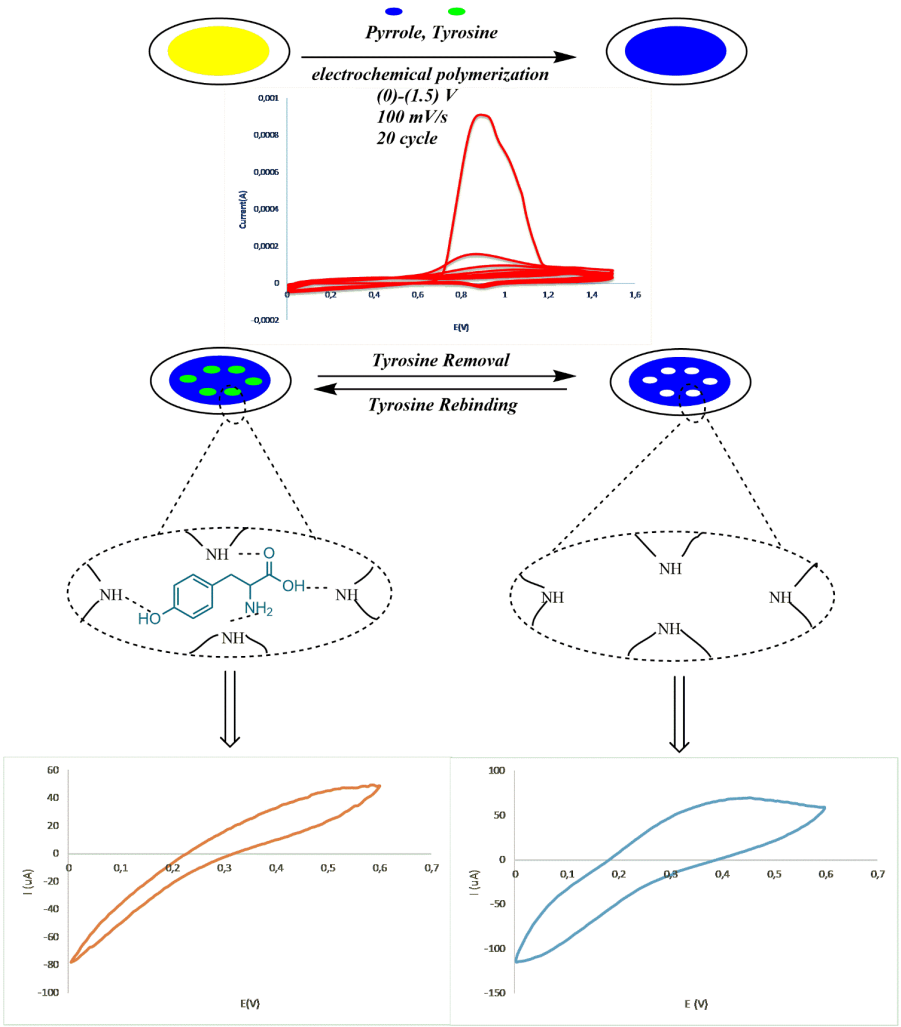

Scheme 1. Preparation of molecularly imprinted polypyrrole modified gold electrode.

After electropolymerization, water – alcohol solution (50%, v/v) was used to remove non-reacted template molecules. As a control electrode, a non-molecularly imprinted polymer (NIP) modified electrode was also prepared under the same experimental conditions in the absence of tyrosine. The prepared MIP and NIP electrodes were stored at the room temperature.

2.4. Electroanalytical measurements

A standard three-electrode cell was used for electrochemical measurements, which were carried out in a supporting ferricyanide electrolyte (0.01 mol/L $K_3[Fe(CN)_6]/K_4[Fe(CN)_6]$ (1:1) solution) containing 0.1 mol/L KCl. CV measurements were performed over a potential range from 0 to 0.6 V at a scan rate of 100 mV/s. SWV measurements were performed over a potential range from (-0,04) to (0,45) V. AC impedance was measured at a potential of 0.175V over the frequency range from 100 mHz to 100 kHz, using an alternating voltage of 5 mV. All experiments were carried out at room temperature (25 ˚C). A blank solution without tyrosine was used to obtain the blank peak current.

3. RESULTS AND DISCUSSION

3.1. Electropolymerization of pyrrole on the surface of the gold electrode

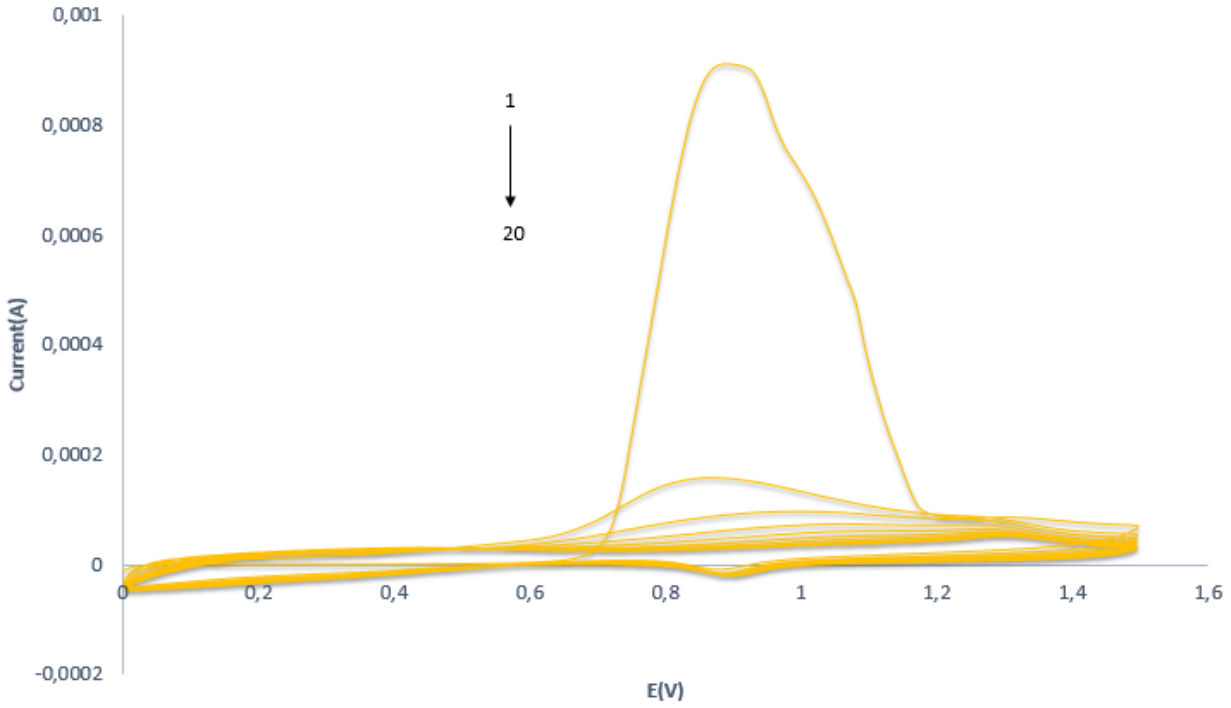

Figure 1. Cyclic voltammograms for the electropolymerization of pyrrole (60 mM) on a gold electrode in pH 5 acetate buffer containing tyrosine (30 mM): scan rate,100mVs^{-1}; number of scans,20.

Cyclic voltammetry was used for electropolymerization of pyrrole on the surface of the gold electrode (Fig. 1). The MIP electrode was prepared as mentioned above. The polymerization solution contained 60 mM Py and 30mM of tyrosine. As the CV showed in Fig 1, in the first scan, an anodic oxidation peak appeared at a potential of 0.9 V, irreversibly. Subsequently, a significant decrease in the anodic oxidation peak during the cycles occurred, which shows the formation of a polymer film onto the surface of electrode. After electropolymerization, a loss of the current response was observed and thought to be arisen from hindrance of redox access to the surface of electrode [13].

3.2. Characterization of tyrosine imprinted electrochemical sensor

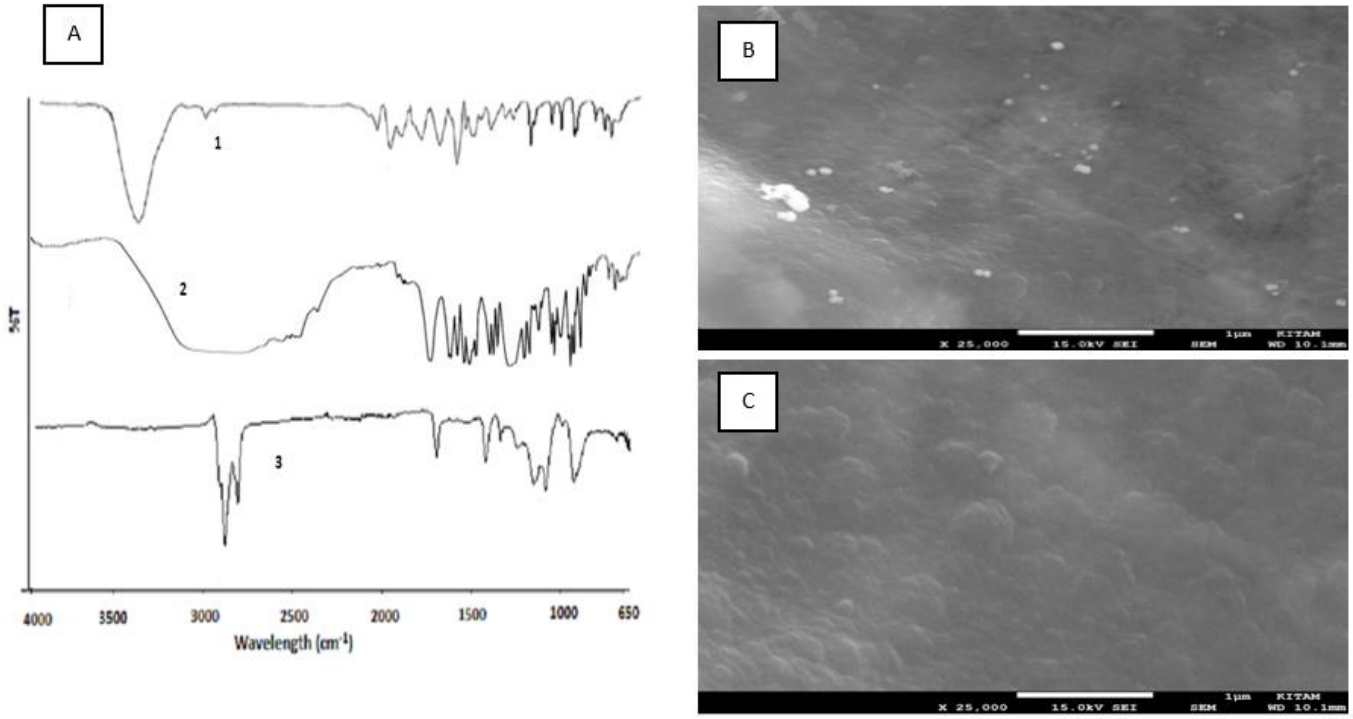

Figure 2. (A) FTIR spectras of 1) polypyrrole 2) tyrosine 3) tyrosine imprinted polypyrrole polymer (B) SEM image of the imprinted electrode (C) SEM image of the non-imprinted electrode.

Figure 2.A shows the FTIR spectra of PPy, tyrosine and the tyrosine imprinted PPy polymer. The peaks 1, 2 and 3 refer to polypyrrole, tyrosine and tyrosine imprinted polypyrrole polymer (Tyr-PPy MIP). The characteristic peaks around 1600 cm^{-1} correspond to the C=C stretching, whereas peaks around 1303 cm^{-1} and 1033 cm^{-1} represent respectively, C-N and C–H bonds. The vibration bands observed at 1300 cm^{-1} and 1036 cm^{-1} are due to C-H in-plane stretching and C-H vibration of 2,5-substituted pyrrole. The occurrence of a peak at 3436 cm^{-1} is assigned to the presence of N–H stretching vibrations [14, 15]. On the second peak the broad absorption band between 2000 and 3500 cm^{-1} is related with overlapping of absorption peaks due to O-H vibration of carboxylic and phenolic O-H and N-H bending vibration of NH_3^+ [16]. On the third peak, N-H absorption peak at 3436 cm^{-1} and the broad envelop, which is occurred through the overlapping of O-H stretch of -COOH and a phenolic and N-H stretch of NH_3^+, cannot be observed. Instead of this, little shoulder formation at

3675 cm^{-1} can be related to polymeric hydrogen bond. The carbonyl peak at 1737 cm^{-1} and C-N stretching peak at 1122 cm^{-1} show that amine and carbonyl groups of amino acid are preserved and polymeric structure is formed through the bond between the hydroxyl group of amino acid and nitrogen of pyrrole.

The SEM characterization is used to investigate the morphology of the imprinted surface. On Fig.2.B and C, the surface of the tyrosine imprinted and non-imprinted polypyrrole modified Au electrodes are seen, respectively. Imprinted tyrosine molecules were observed on the polypyrrole modified gold surface.

3.3. Electrochemical characterization of modified electrode

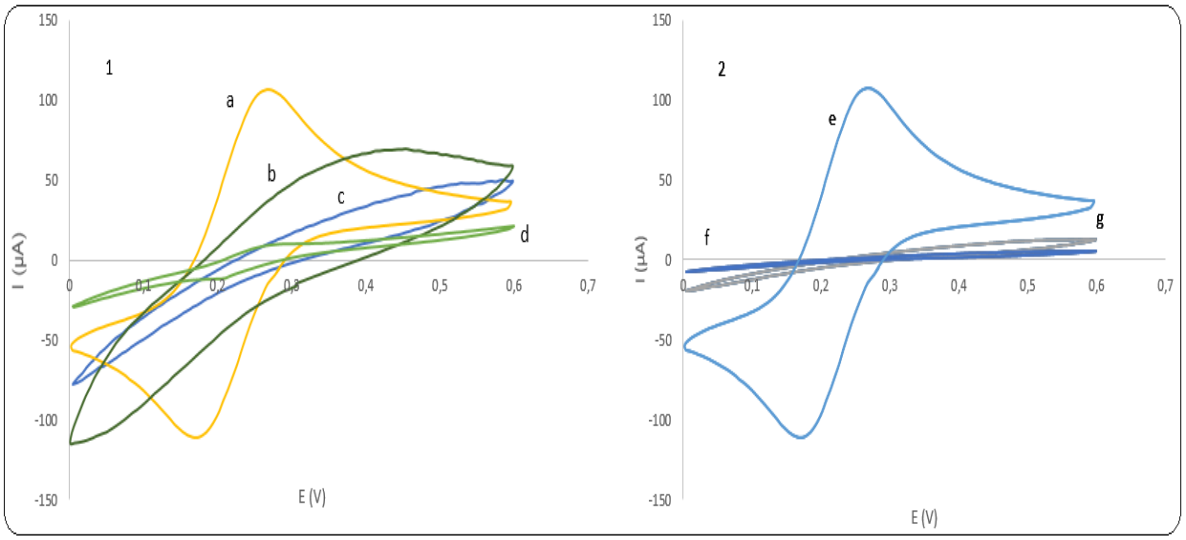

Figure 3. 1) CV curves of MIP electrode under different conditions: a) bare electrode; b) MIP electrode after Tyr removal c) MIP electrode; d) MIP electrode after interaction with Tyr; 2) CV curves of NIP electrode under different conditions: e) bare electrode; (f) NIP electrode; (g) NIP electrode after interaction with Tyr.

For electrochemical characterization of MIP and NIP electrodes, cyclic voltammetry (CV) and electrochemical impedance spectroscopy (EIS) were used. Cyclic voltammograms were recorded in the presence of $[Fe(CN)_6]^{3-}/[Fe(CN)_6]^{4-}$ in 0.1mol/L KCl as a probe. As shown in Fig. 3.1, in which a refers to the bare electrode and c refers to the electrode after electropolymerization. After electropolymerization, polymer film hindered the occurrence of a redox reaction, which caused current reduction. The process from c to b refers to template removal. After tyrosine removal, the spesific cavities allow the redox reaction of $[Fe(CN)_6]^{3-}/[Fe(CN)_6]^{4-}$ so there has been a current increase. After tyrosine binding, shown as d, the tyrosine specific cavities were reoccupied, and this caused a smaller current than the removal current, b.

On the contrary, NIP electrode did not show any significant current change despite interaction with template (Fig. 3.2.f-g). This indicates that NIP electrode failed to recognize tyrosine.

For probing the feature changes of a modified electrode surface, electrochemical impedance

spectroscopy (EIS) is an efficient method [17]. Under same circumstances as CV, this technique was used to confirm that the MIP modified electrode was prepared properly.

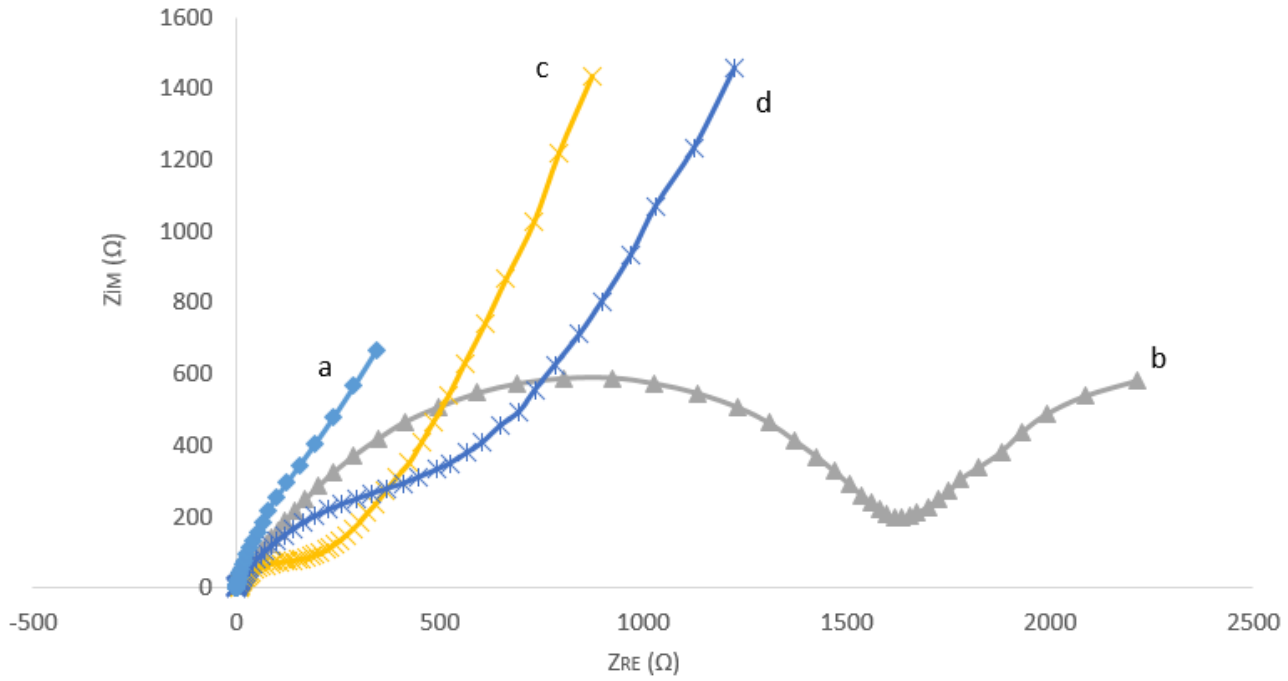

Figure 4. Impedance spectra of gold electrode under different conditions; (a) bare electrode; (b) MIP modified; (c) MIP electrode after removal of Tyr; (d) MIP electrode after interaction with Tyr.

Fig. 4 shows the changes in MIP formation, template elution and interaction with template, as shown in b,c,d, respectively and a refers to the bare Au electrode surface. The diameter of semicircle refers to electron transfer resistance (R_{et}) and with the formation of MIP film, surface of Au electrode was covered with polymeric film, and this caused resistance increase, as can be seen clearly from curve a to b. [18]. The prepared polymeric film acted as an insulating layer, which blocks electron transfer between the electrolyte and the electrode during analysis. After this through template removal there had been a resistance decrease, from curve b to c. This could be related with the successful extraction of Tyr from the imprinted polymer, which allow electron transfer between the electrolyte and the electrode easily. After template removal, electrode was interacted with tyrosine solution and resistance was increased, as can be observed from curve c to d. This increase arises from rebinding of tyrosine, which restricts electron transfer between the electrode and the electrolyte. In a study, after interaction with template molecule, the impedance of the surface was increased due to reoccupation of cavities in the imprinted polymer. This increase was reported as electron transfer resistance due to the restriction of electron transfer between the electrode and the electrolyte, as in our study [19]. According to experimental and literature data it can be implied that the polymer membrane had recognition sites for Tyr and MIP film was prepared properly.

3.4. Optimization of Experimental Conditions

3.4.1. Effect of tyrosine concentration

The effect of the template concentration was tested on the response of the resulting Tyr imprinted polypyrrole electrode to Tyr. One of the factors affecting sensor response is the template concentration in the polymerization mixture. Template concentration is directly related to with the recognition sites in molecularly imprinted polymer [20]. In the presence of a constant concentration of pyrrole (60 mM), different concentrations of tyrosine were tested for the optimum template concentration in the polymerization mixture. As can be seen in Fig. 5A the peak current change of MIP electrode increased with increasing concentration of tyrosine to 30 mM. After this concentration current change decreased. Because of this 30 mM Tyr was selected as optimum template concentration.

3.4.2. Polymerization cycle number of Pyrrole

The response of the imprinted sensor can be influenced by the thickness of the imprinted membrane and the imprinted sites. The polymer thickness can be adjusted through the number of electropolymerization cycle and it is important in terms of imprinted sites. With the increase of membrane thickness, it could be hard to reach to the imprinted sites because of mass transfer resistance [21].

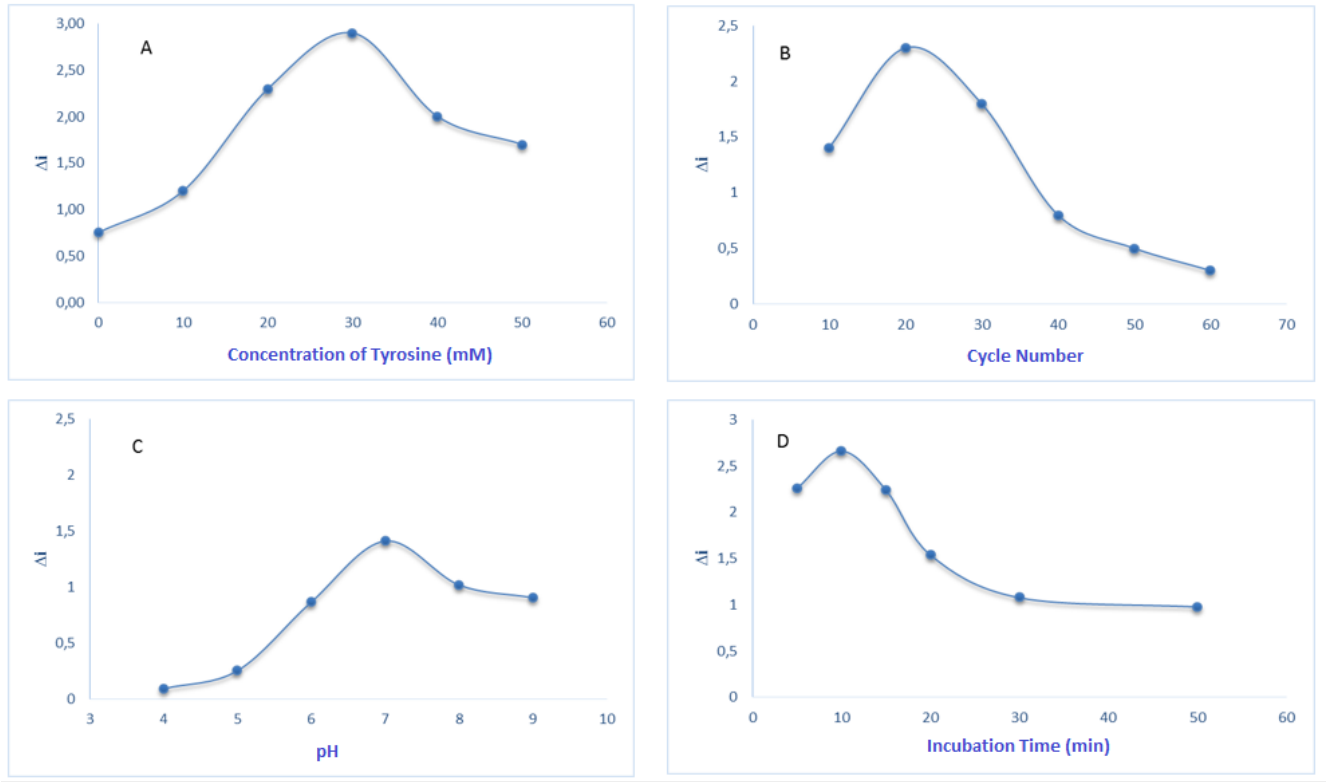

Figure 5. Effect of different parameters on the response of the MIP. (A) Effect of different concentration of tyrosine in electropolymerization process. (B) Effect of the number of cycles in electropolymerization process. (C) Effect of pH. (D) Effect of incubation time.

As shown in Fig.5.B it was observed that the peak current increased and reached a maximum with 20 cycles, and then decreased at higher cycles. Thus, in this work, it was decided that 20 cycles could bring out an optimum membrane thickness to provide the highest sensitivity to tyrosine.

3.4.3. Effect of pH

The pH of the solution in adsorption step has a significant influence on the tyrosine oxidation at the surface of the modified electrode. Therefore, the effect of medium pH was analyzed with a series of convenient buffer solutions in a varying pH range between 4.0-9.0. As shown in Fig.5.C the current intensity of the oxidation peak reaches its maximum at a pH value of 7, and then decreased as the pH increases further. The reason may be that in high alkalinity the tyrosine was formed in anionic structure and the stability of the imprinted film will be defected [18]. Therefore, pH 7 was chosen as the suitable pH for further studies.

3.4.4. Incubation Time

Template molecules were removed from the imprinted film with 1 M HCl solution after that the molecularly imprinted electrode has interacted with 10 µM Tyr solution in different times and the change of the peak current was drawn vs. the incubation time (Fig.5.D). The results show that the peak current decreased rapidly (increase in ΔI) with the increase in the incubation time. Maximum response was obtained after 10 min, suggesting that the incubation equilibrium was reached. Thus, the optimum incubation time of 10 min was chosen.

3.5. Performance of the modified sensor

3.5.1. SWV response and analytical curve

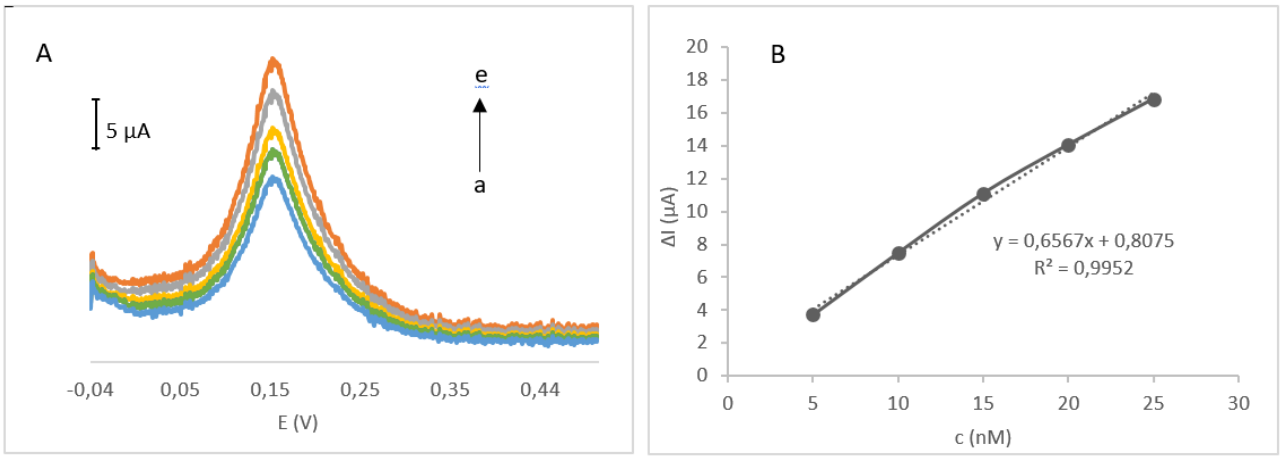

Figure 6. (A) Square wave voltammograms of the imprinted Au electrode with different tyrosine concentration in pH 7.0 phosphate buffer, tyrosine concentration was (a) 5, (b) 10, (c) 15, (d) 20, (e) 25 nM, (a→e), respectively. (B) The calibration curve of tyrosine.

In this study, quantitative analysis of tyrosine using the proposed MIP electrode under optimized experimental conditions was performed using SWV. After the template removal, MIP-modified electrodes were dipped into the tyrosine solutions at different concentrations between 5 and 25 nM. After dipping for 10 min, SWV analyses were made. As shown in Fig. 6.A, the peak current response increased with increasing concentrations of tyrosine in phosphate buffer (pH=7). Under the optimized conditions, a linear relationship is obtained between current response and tyrosine concentration in the range of 5×10^{-9} to $2{,}5\times10^{-8}$ M as can be seen in Table 1.

Table 1. Features of calibration plot (n=3)

Regression equation	I (μA) = 0.6567x + 0.8075*
Correlation coefficient (r)	0.9952
Linearity range (M)	$5.0 \times 10^{-9} – 2.5\times10^{-8}$
LOQ (M)	8.2×10^{-9}
LOD (M)	2.5×10^{-9}

*y=ax+b; y, current change; x, Tyr concentration; a, slope; b, intercept; LOD, limit of detection; and LOQ, limit of quantification.

The correlation coefficient is 0.9952 (Fig 6.B). The linear regression equation is I (μA) = 0.8075 + 0.6567x c (μM). The detection limit was calculated to be 2.5×10^{-9} M, which was lower than that reported in some other methods, as shown in Table 2.

Table 2. Comparison of the performance of developed sensor with other developed sensors

Detection Method	Modification	Linear Range (M)	Limit of Detection (M)	References
DPV	Poly(thionine) GCE	$1x10^{-6}$ - $2.5x10^{-4}$	$5.7x\ 10^{-5}$	[2]
CV	Fe-HA/tyrosinase GCE	$1x10^{-7} – 1x10^{-5}$	$2.45x10^{-7}$	[22]
CV	Graphene Oxide	$5x10^{-7} – 2x10^{-5}$	$7.5x10^{-8}$	[23]
CV	Diamond Nanowire	$1x10^{-6} – 1x10^{-4}$	$0.2x10^{-6}$	[24]
SWV	MIP-polypyrrole	$5x10^{-9} – 2.5x10^{-8}$	$2.5x\ 10^{-9}$	This study

3.5.2. Selectivity, repeatability, and stability of the sensor

The selectivity of the imprinted electrode to tyrosine was evaluated by SWV with the other three similar molecules, phenylalanine, histidine, and L-3,4-dihydroxyphenylalanine (L-DOPA). After template removal, MIP modified electrodes were immersed separately in 10 μM solutions of these above-mentioned molecules. As shown in Fig. 7.A, the current response of the imprinted electrode toward tyrosine was about 10, 4 and 6 times higher than that of histidine, phenylalanine and DOPA. However, the adsorption capacity of NIP modified electrode was almost the same for each molecule as

can be seen in Fig.7. B. The good specifity arised from the cavities which match the shape of tyrosine during the electropolymerization process.

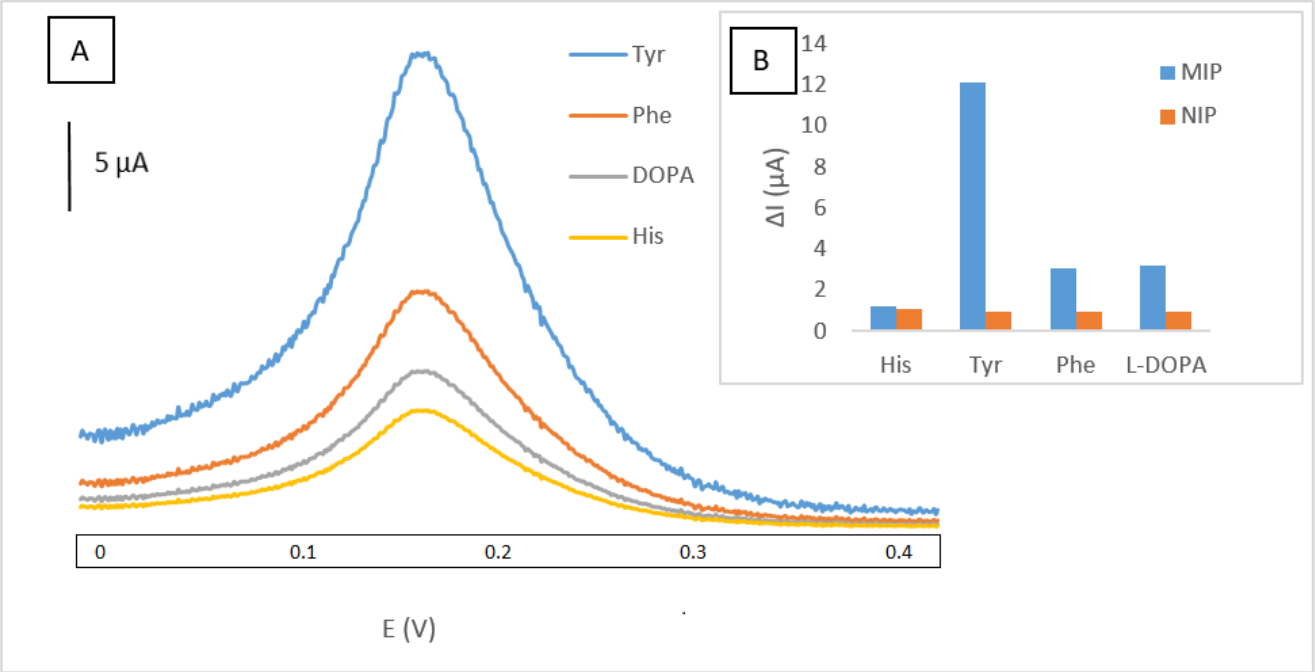

Figure 7. (A) Square wave voltammograms of the imprinted Au electrode with different molecules in pH 7.0 phosphate buffer. (B) Difference between NIP and MIP modified electrodes under same conditions.

The electrodes were washed after 10 min incubation and placed in phosphate buffer solution for SWV scanning. According to the obtained peak currents, MIP sensor had weak specificity for other structural analogs and tyrosine selectivity, due to its complementary cavities for Tyr.

Upon optimization, this sensor detected 5 nM tyrosine nine times. After each measurement, the electrode was washed with 1M HCl solution to remove the template molecules. Its relative standard deviation (RSD) was 2.1%, indicating that repeatability of this sensor is good. Meanwhile, the parallel determination was conducted five times every other day. The peak current was reduced to 5.6% within 10 days, which indicates good sensor stability.

3.5.3. Determination of L-Tyrosine in Plasma Samples

The prepared imprinted sensor was successfully applied for the detection of tyrosine levels in a human plasma sample, which is obtained from Ondokuz Mayıs University Hospital. The samples were directly used after dilution a hundred times with PBS (pH 7.4). This study was made using a standard addition method and concentration calculated by extrapolation.

Table 3. Determination of tyrosine in human plasma samples (n=3)

Sample	Added (nM)	Found (nM)	Recovery (%)	RSD(%)
1	-	43.6	-	-
2	20	68.3	107.4	2.1
3	40	89.0	106.5	1.6
4	60	112.5	108.5	2.2

The data given in Table 3 shows the results for detection of tyrosine human plasma samples. The samples were frozen and stored at -20 °C until used.

4. CONCLUSIONS

In this study a novel imprinted electrochemical sensor, based on imprinting technique was fabricated for the direct determination of tyrosine by using tyrosine as template molecule and pyrrole as functional monomer, without any necessity to other reagents. The designed electrochemical sensor exhibited good sensitivity, selectivity for tyrosine and obtained good reproducibility and repeatability. Moreover, the developed sensor can be successfully used in real samples with the high recovery and low RSD values.

CONFLICT OF INTEREST
The author(s) declare(s) that there is no conflict of interest regarding the publication of this paper.

References

1. S. B. Revin, S. A. John, *Sens Actuators* B, 161 (2012) 1059.
2. M. Rahman, N. S. Lopa, K. Kim and J. J. Lee, *J. Electroanal. Chem*., 754 (2015) 87.
3. H. Orhan, N. Vermeulen, C. Tump, H. Zappey and J. Meerman, *J. Chromatogr*. B, 799 (2004) 245.
4. X. Mo, Y. Li, A. Tang and Y. Ren, *Clin. Biochem*., 46 (2013) 1074.
5. Y. Huang, X. Jiang, W. Wang, J. Duana and G. Chen, *Talanta*, 70 (2006) 1157.
6. G. Vasapollo, R. Sole, L. Mergola, M. Lazzoi, A. Scardino, S. Scorrano and G. Mele, *Int. J. Mol. Sci.*, 12 (2011) 5908-5945.
7. B. Schweiger, J. Kim, Y.J. Kim and M. Ulbricht, *Sensors*, 15 (2015) 4870-4889.
8. L. Özcan, M. Sahin and Y. Sahin, *Sensors*, 8 (2008) 5792.
9. B. Rezaei, B. M. Khalili and A. A. Ensafi, *Biosens. Bioelectron*., 15 (2014) 77.
10. L. Ozcan., Y. Sahin, *Sens. Actuators* B, 127 (2007) 362–369.
11. A. Ramanavicienea, A. Ramanavicius, *Biosens. Bioelectron*., 20 (2004) 1076.
12. A. Ramanavicius, A. Kausait and A. Ramanavicien, *Sens. Actuators* B, 111–112 (2005) 532.
13. K. Kor, K. Zarei, *Talanta*, 146 (2016) 181.
14. M. Chougulea, S. G. Pawara, P. R. Godsea, R. Mulika, S. Senb and V.B. Patila, *Soft Nanoscience Letters*, 1 (2011) 6.
15. S. Liu, M. Oliveira, *Mat. Res*., 10 (2007) 205.
16. P. Anandan, S. Vetrivel and S. Karthikeyan, *Optoelectron. Adv. Mat*., 6 (2012) 1128.
17. J. Li, J. Zhao and X. Wei, *Sens. Actuators* B 140 (2009) 663.

18. J. Zhang, C. Wang, Y. Niu, S. Lib and R. L. School, *Sens. Actuators* B, 249 (2017) 747–755.
19. B. Rezaei, O. Rahmanian and A. A. Ensafi, *Sens. Actuators* B, 196 (2014) 539–545.
20. Y.T. Liu, J. Deng, X. L. Xiao, L. Ding, Y. L. Yuan, H. Li, X.T. Li, X.N. Yan and L.L. Wang, *Electrochim. Acta*, 56 (2011) 4595.
21. L. Kong, X. Jiang, Y. Zeng, T. Zhou and G. Shi, *Sens. Actuators* B, 185 (2013) 424.
22. P. Kanchana, N. Lavanya and C. Sekar, *Mat. Sci. Eng*. C, 35 (2014) 85.
23. J. Wei, J. Qiu, L. Li, L. Ren, X. Zhang, J. Chaudhuri and S. Wang, *Nanotechnology*, 23 (2012) 335.
24. Q. Wang, A. Vasilescu, P. Subramanian, A. Vezeanuc, V. Andreic, Y. Coffinier, M. Li, R. Boukherroub and S. Szunerits, *Electrochem Commun*., 35 (2013) 84.